

Speed of Sound and Ideal-Gas Heat Capacity at Constant Pressure of Gaseous Difluoromethane

Li-Qun Sun, Yuan-Yuan Duan, Lin Shi, Ming-Shan Zhu,* and Li-Zhong Han

Thermal Engineering Department, Tsinghua University, Beijing 100084, People's Republic of China

The speed of sound of gaseous difluoromethane (HFC-32) was measured for temperatures from 273.15 K to 333.15 K and pressures from 48 kPa to 390 kPa with a cylindrical, variable-path acoustic interferometer operating at 156.252 kHz. The uncertainty of the speed of sound was less than $\pm 0.1\%$. The ideal-gas heat capacity at constant pressure and the second acoustic virial coefficients were determined over the temperature range from the speed of sound measurements. The ideal-gas heat capacity at constant pressure results and second virial coefficients calculated from these speed of sound measurements were compared with results from the literature determined from *PVT* measurements and from speed of sound measurements. The uncertainty of the ideal-gas heat capacity at constant pressure was estimated to be less than $\pm 1\%$.

Introduction

Difluoromethane (HFC-32) is considered as the most important candidate to replace chlorodifluoromethane (HCFC-22) by mixing with other HFCs, e.g., HFC-125 and/or HFC-134a. However, measurements of the speed of sound and the ideal-gas heat capacity of gaseous HFC-32 are limited. Hozumi et al. (1994) measured the speed of sound in HFC-32 for temperatures from 273 K to 343 K and pressures from 20 kPa to 250 kPa and determined the ideal-gas heat capacity. Defibaugh et al. (1994) reported the ideal-gas heat capacity of HFC-32 from 200 K to 400 K. TRC (V-6880 (NH) 1989) gave the ideal-gas heat capacity up to 3000 K. McLinden (1990) gave the correlation of the ideal-gas heat capacity over the temperature range from 150 K to 500 K. In this paper, the speed of sound in HFC-32 for temperatures from 273.15 K to 333.15 K and pressures from 48 kPa to 390 kPa was measured with an uncertainty of $\pm 0.1\%$. The ideal-gas heat capacity at constant pressure at the corresponding temperatures was determined with an uncertainty of $\pm 1\%$. The second virial coefficients were calculated from the speed of sound measurements and compared with those determined with *PVT* measurements and speed of sound measurements.

Working Equation

The relationship between the speed of sound W and the isentropic compressibility is given by

$$W^2 = (\partial p / \partial \rho)_s \quad (1)$$

From thermodynamics, the acoustic virial expansion is given by

$$W^2 = (\gamma_0 RT/M)[1 + (\beta_a/RT)p + (\gamma_a/RT)p^2 + \dots] \quad (2)$$

The ideal-gas heat capacity at constant pressure, C_p^0 , can be determined from

$$C_p^0 = R\gamma_0/(\gamma_0 - 1) \quad (3)$$

The subscript, s , in eq 1 refers to an isentropic process, M is the molar mass of the sample gas, p is the gas

pressure, T is the gas temperature, R is the universal gas constant, γ_0 is the zero-pressure limit of the heat capacity ratio, and β_a and γ_a are the second and third acoustic virial coefficients of the gas. The speed of sound was measured as a function of pressure at constant temperatures and at low pressures. The coefficient $(\gamma_0 RT/M)$ was then determined by a least-squares regression. If both T and M are known, the heat capacity ratio, γ_0 , can be obtained.

Experimental Instrument

The experimental instrument, which was described previously (Zhu, 1993), will be introduced again briefly here. The schematic of the entire measuring system is shown in Figure 1. A steel pressure vessel was used in the instrument to maintain the pressure. The vessel consisted of a cylinder with two pistons at opposite ends of the cylinder. One piston, equipped with an emitting transducer, was fixed, while the other one, equipped with a reflector, could slide freely in the cylinder. The reflector also operated as a detector. The transducer was made of piezoelectric crystal. Its operating frequency had a variation of ± 1 Hz. The vessel was suspended in a stirred fluid bath during the course of the experiment. The temperature uncertainty was less than ± 10 mK. The pressures of the gas sample were measured with a dead-weight tester and a differential pressure transducer with an uncertainty of ± 500 Pa. During the experiments, the movable transducer was slid relative to the fixed transducer. The wave emitted by the fixed transducer and the wave reflected by the free transducer will interfere with each other when the distance between the two transducers is some integer multiple of half the wavelength. Once the changed distance, l , of the movable transducer and the number of the interference, N , are measured, the wavelength, λ , can be determined according to the principle of ultrasonic interference. Then the speed of sound in the test gas sample can be determined with the wavelength, λ , and the sound frequency, f . The frequency of the sound wave emitted from the piezoelectric crystal transducer is essentially constant, because the resonating frequency of the crystal is nearly independent of the environment (Zhu, 1993). Thus, the precision of the determination of the speed of sound depends mainly on the precision of the wavelength measurement. The precision of the wavelength measurements was improved by moving the piston more than 30 wavelengths in this work. A

* Author to whom correspondence should be addressed. E-mail: dmc@mail.tsinghua.edu.cn.

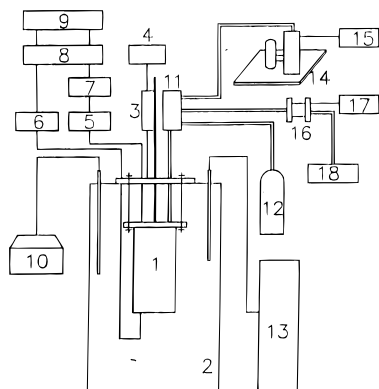


Figure 1. Schematic of the speed of sound measuring system: 1, main body; 2, thermostat; 3, 4, displacement measuring system; 5, generator; 6, amplifier; 7, frequency meter; 8, wave indicator; 9, phase detector; 10, temperature acquisition unit; 11, three-way valve; 12, gas sample bottle; 13, temperature controller; 14, vacuum pump; 15, vacuum meter; 16, differential pressure detector; 17, digital pressure detector; 18, dead-weight tester.

discussion of the uncertainty in the experiment has been described in detail in the previous publication (Zhu, 1993). The instrument was checked with argon, and the measured results showed that the uncertainty of the speed of sound measured with this instrument is less than $\pm 0.1\%$ and the uncertainty of the ideal-gas heat capacity at constant pressure determined with the measured speed of sound is less than $\pm 1\%$.

Results and Analysis

Wavelength measurements for HFC-32 were made along 10 isotherms between 273.15 K and 333.15 K. The maximum pressure along the isotherms was about 400 kPa, which is below 30% of the saturated vapor pressure of HFC-32 at the corresponding temperatures. The mass purity of the used HFC-32 sample is 99.95%.

The speed of sound of HFC-32 was obtained from the corrected wavelengths together with the fixed frequency. The measurement values were corrected for diffraction and guided mode dispersion (He and Zhao, 1980) using the empirical equation

$$\Delta\lambda_{\text{dg}} = \lambda[\alpha_2(\lambda/D)^4 + \alpha_3(\lambda/D)^6] \quad (4)$$

where λ is the wavelength, D is the diameter of the resonance tube (75.04 mm in this work), $\alpha_2 = 0.3806$, and $\alpha_3 = 79.74$.

The measured speed of sound was corrected for absorption dispersion using the Kirchhoff Helmholtz (boundary layer) absorption coefficient α_{KH} and the classical absorption coefficient α_{CL} . According to the boundary layer theory (He and Zhao, 1980)

$$\alpha_{\text{KH}} = [2/(DW)]\{\nu^{0.5} + (\gamma - 1)(\kappa/\rho C_p)^{0.5}\}(0.5\omega)^{0.5} \quad (5)$$

where D is the tube diameter, W is the speed of sound, ν is the kinematic viscosity of the sample gas, κ is the thermal conductivity, C_p is the heat capacity at constant pressure, ρ is the density, ν is the ratio of the principal heat capacity, and ω is the angular frequency.

The classical absorption coefficient α_{CL} is given by two parts: the thermal conductivity and the shear viscosity (He and Zhao, 1980)

$$\alpha_{\text{CL}} = K(1 - \gamma)\omega^2/(2\rho W^3 C_v) + 2\omega^2\eta/(3W^3\rho) \quad (6)$$

where C_v is the heat capacity at constant volume and the other parameters are the same as for the last equation.

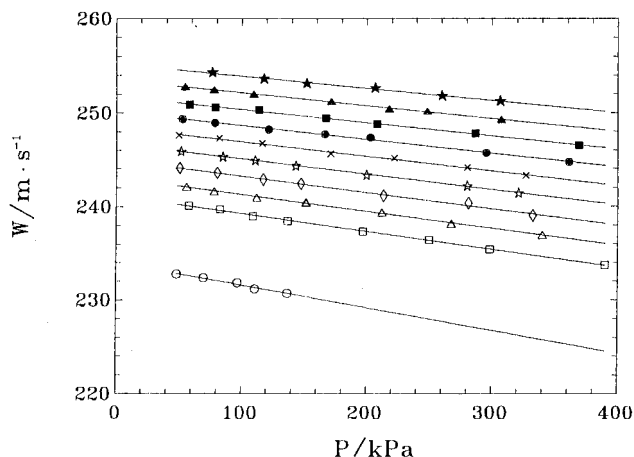


Figure 2. Obtained speed of sound versus temperatures in HFC-32: (○) 273.15 K; (□) 293.15 K; (△) 298.15 K; (◇) 303.15 K; (☆) 308.15 K; (×) 313.15 K; (●) 318.15 K; (■) 323.15 K; (▲) 328.15 K; (★) 333.15 K; (—) calculated from eq 11.

Table 1. Speed of Sound Data for HFC-32

T/K	P/kPa	$W/(\text{m}\cdot\text{s}^{-1})$	T/K	P/kPa	$W/(\text{m}\cdot\text{s}^{-1})$
273.15	136.72	230.695	273.15	69.75	232.357
	110.82	231.152		48.34	232.762
	96.76	231.817			
293.15	389.67	233.709	293.15	136.72	238.448
	298.39	235.405		108.90	238.988
	250.01	236.403		82.69	239.718
	196.99	237.320		57.63	240.105
298.15	340.24	236.920	298.15	112.15	240.927
	267.63	238.143		77.92	241.640
	212.20	239.331		55.96	242.099
	151.36	240.461			
303.15	332.72	238.993	303.15	117.21	242.851
	281.51	240.312		80.43	243.554
	213.62	241.130		50.49	244.072
	147.48	242.395			
308.15	321.35	241.416	308.15	110.76	244.894
	280.39	242.175		84.97	245.292
	200.01	243.325		51.58	245.874
	143.28	244.306			
313.15	327.07	243.240	313.15	116.22	246.700
	280.40	244.086		82.08	247.251
	222.05	245.101		49.59	247.584
	170.96	245.593			
318.15	361.29	244.672	318.15	121.55	248.189
	295.45	245.650		78.60	248.916
	202.82	247.318		52.53	249.343
	166.62	247.671			
323.15	368.90	246.471	323.15	113.56	250.326
	286.76	247.761		78.73	250.583
	208.28	248.753		58.38	250.910
	167.31	249.399			
328.15	307.51	249.253	328.15	109.57	251.993
	248.34	250.157		77.84	252.455
	217.89	250.435		54.65	252.789
	171.55	251.204			
333.15	306.59	251.229	333.15	152.03	253.113
	260.24	251.793		117.84	253.612
	206.87	252.637		76.66	254.293

The shear viscosity, η , required to determine the absorption was calculated from a modified Eucken equation (Reid and Herwood, 1966)

$$\eta = KM/(1.77 + 1.33C_v/R) \quad (7)$$

The correction is then

$$\Delta\lambda_{\text{ab}} = \lambda^2(\alpha_{\text{KH}} + \alpha_{\text{CL}})[1 + \lambda(\alpha_{\text{KH}} + \alpha_{\text{CL}})/\pi]/2\pi \quad (8)$$

For polyatomic molecules, vibrational relaxation has the most important impact on the speed of sound measure-

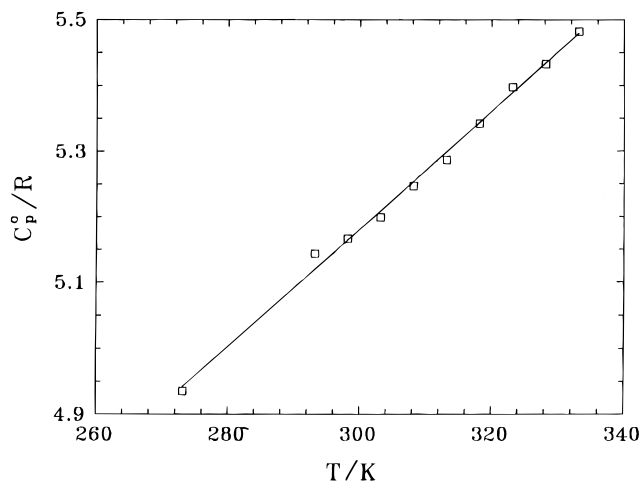


Figure 3. Obtained ideal-gas heat capacity at constant pressure of HFC-32 versus temperature: (—) calculated from eq 12.

Table 2. Ideal-Gas Heat Capacity at Constant Pressure and Second Acoustic Virial Coefficient for HFC-32

<i>T</i> /K	C_p^0/R	$\beta_a/(\text{cm}^3 \cdot \text{mol}^{-1})$	<i>T</i> /K	C_p^0/R	$\beta_a/(\text{cm}^3 \cdot \text{mol}^{-1})$
273.15	4.9349	-466.13	313.15	5.2862	-325.82
293.15	5.1434	-382.83	318.15	5.3419	-312.71
298.15	5.1666	-365.39	323.15	5.3972	-301.35
303.15	5.1988	-353.24	328.15	5.4324	-295.91
308.15	5.2466	-335.58	333.15	5.4820	-279.21

ments. Its correction can be calculated as (He and Zhao, 1980)

$$\Delta\lambda_{\text{vib}} = \lambda \frac{C_{v0}(C_{v0} + r) + C_{v1}(C_{v1} + r)(\omega\tau)^2}{2[C_{v0}^2 + C_{v1}^2(\omega\tau)^2](1 + r/C_{v0})} \quad (9)$$

where C_{v0} is the heat capacity at zero frequency, $r = C_p - C_{v1}$, $C_{v1} = C_{v0} - C_{\text{vib}}$, and C_{vib} is $(C_{p,m} - 4R)$, the vibrational contribution to the heat capacity. The three corrections for the wavelength are then combined as

$$\lambda_c = \lambda - (\Delta\lambda_{\text{dg}} + \Delta\lambda_{\text{ab}} + \Delta\lambda_{\text{vib}}) \quad (10)$$

In eqs 4–10, all the thermodynamical properties are calculated with the NIST program Refprop, Version 4.01, having an estimated accuracy of 1% (Gallagher, 1989).

The corrected speed of sound results for gaseous HFC-32 are listed in Table 1.

The measured speed of sound results along each isotherm was correlated as a function of pressure with the following linear squared function

$$W^2 = A_0 + A_1 p \quad (11)$$

where A_0 and A_1 are numerical constants for each isotherm. Figure 2 shows the speed of sound versus pressure along each isotherm. The data for the ideal-gas heat capacity at constant pressure, C_p^0 , and the corresponding values of β_a are listed in Table 2. Figures 3 and 4 show the data for C_p^0 and β_a as a function of temperature. The ideal-gas heat capacity at constant pressure and the second acoustic virial coefficient were derived by regression analysis of the present speed of sound measurements. The C_p^0 data was correlated by the following equation

$$C_p^0/R = 2.6716 + 7.7825 \times 10^{-3}(T/K) + 1.93422 \times 10^{-6}(T/K)^2 \quad (12)$$

where R is the universal gas constant. Figure 5 shows the deviations of the measured ideal-gas heat capacity of

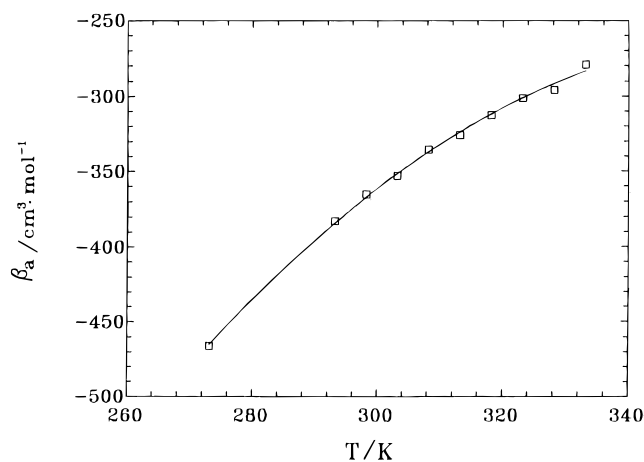


Figure 4. Obtained second acoustic virial coefficient β_a versus temperature: (—) calculated from eq 13.

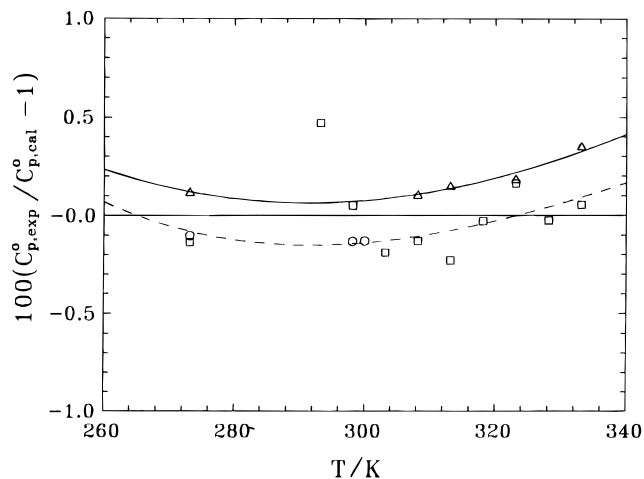


Figure 5. Comparisons of heat capacity by different authors with eq 12: (Δ) data by Hozumi et al.; (\circ) data from TRC database; (\square) data of this work; (—) correlation by Hozumi et al.; (---) correlation by McLinden.

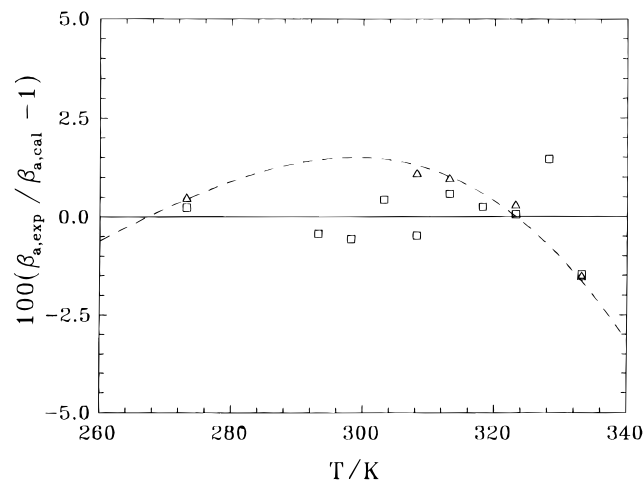


Figure 6. Comparisons of second acoustic virial coefficient β_a by different authors with eq 13: (Δ) data by Hozumi et al.; (\square) data of this work; (---) correlation by Hozumi et al.

constant pressure results from the prediction of eq 12 and from the correlations of different authors. Equation 12 reproduces our data very well with a maximum deviation of less than 0.5%. The root mean square (RMS) deviation using eq 12 is 0.21%. The maximum deviation of the data from other authors with the prediction of eq 12 is also less than 0.5% as shown in Figure 5. The data for C_p^0 obtained by Kubota et al. (1995) with a flow calorimeter differ

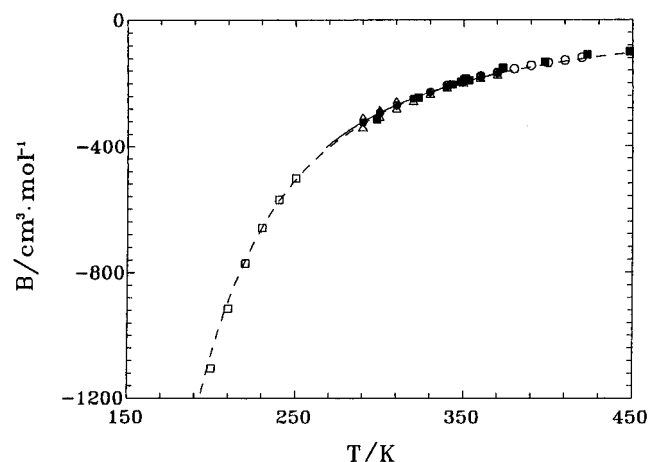


Figure 7. Second virial coefficient B calculated with eq 18: (□) data by Weber et al.; (△) data by Qian et al.; (○) data by Sato et al.; (◇) data by Bignell et al.; (■) data by Kuznetsov et al.; (●) data by Zhang et al.; (—) correlation by Defibaugh et al.; (---) calculated from eq 18.

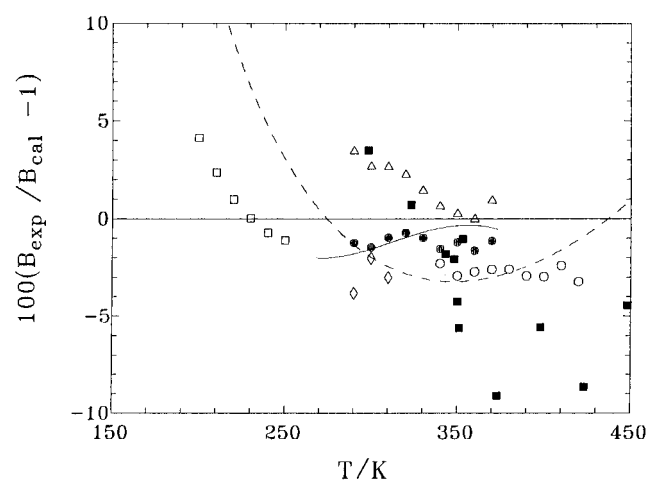


Figure 8. Deviations of second virial coefficient data by different authors from eq 18: (□) data by Weber et al.; (△) data by Qian et al.; (○) data by Sato et al.; (◇) data by Bignell et al.; (■) data by Kuznetsov et al.; (●) data by Zhang et al.; (—) correlation by Defibaugh et al.; (---) correlation by Hozumi et al.

significantly from eq 12 with a minimum deviation exceeding 10%. For this reason, these results were not shown in Figure 5. The broken curve shows a correlation developed by McLinden (1990) on the basis of spectroscopic data from Rodgers et al. (1974) and JANAF (1985).

The β_a data was correlated with

$$\beta_a/\text{cm}^3\cdot\text{mol}^{-1} = -3.56721 \times 10^3 + 18.1864(T/\text{K}) - 2.50024 \times 10^{-2}(T/\text{K})^2 \quad (13)$$

The RMS deviation of eq 13 is 0.79%. The maximum deviation of the present data from eq 13 is 1.5%. The β_a data and correlation from different authors are compared with eq 13 in Figure 6. It can be seen that all the data and the correlation are consistent with eq 13 with a maximum deviation of less than 2.5%.

The thermodynamic relation between β_a and B is given by

$$\beta_a = 2B + 2(\gamma_0 - 1)T \frac{dB}{dT} + \frac{(\gamma_0 - 1)^2}{\gamma_0} T^2 \frac{d^2B}{dT^2} \quad (14)$$

where γ_0 is the ideal-gas heat capacity ratio. This equation was obtained using the square-well potential for the intermolecular force. We adopted a semiempirical method

to solve this second-order differential equation. This procedure is similar to that described in detail in Ewing et al. (1987, 1988, 1989).

For the second virial coefficient, the square-well model leads to the simple equation (Hirschfelder and Curtiss, 1954)

$$B(T) = b_0[1 - (r^3 - 1)\Delta] \quad (15)$$

with

$$\Delta = \exp(\epsilon/kT) - 1 \quad (16)$$

Equations 14–16 include three parameters to be fit to the data; the covolume b_0 , the scaled well depth ϵ/k , and the ratio of the radius of the well to the radius of the hard core r . From eq 14, the corresponding expression for β_a is

$$\beta_a/2b_0 = r^3 + \left[-1 + \frac{(\gamma_0 - 1)}{\gamma_0} \frac{\epsilon}{kT} - \frac{(\gamma_0 - 1)^2}{2\gamma_0} \left(\frac{\epsilon}{kT} \right)^2 \right] (r^3 - 1) \exp(\epsilon/kT) \quad (17)$$

The numerical constants in this equation were determined by trial-and-error analysis using the present β_a values and the equation for C_p^0 . The regression analysis led to the following parameters: $\beta_0 = 32.82 \text{ cm}^3\cdot\text{mol}^{-1}$, $\epsilon/k = 670.0 \text{ K}$, and $r = 1.30288$. The second virial coefficient, B , was correlated as

$$B/\text{cm}^3\cdot\text{mol}^{-1} = 32.82[1 - 1.212(e^{670/T} - 1)] \quad (18)$$

Figure 7 shows the second virial coefficient, B , versus the temperature for a temperature range from 190 K to 450 K calculated with eq 18 along with experimental data obtained by different authors. The calculated values of B from eq 18 for gaseous HFC-32 are compared with available experimental data and correlations by Weber and Goodwin (1993), Qian et al. (1993), Sato et al. (1994), Kuznetsov and Los (1985; from TRC source, 1996), Bignell and Dunlop (1993; from TRC source 1996), Defibaugh et al. (1994), Hozumi et al. (1994), and Zhang et al. (1995) in Figure 8. The differences between the present correlation and the experimental data for B by Weber and Goodwin (1993), Qian et al. (1993), and Bignell and Dunlop (1993; from TRC source 1996) are less than 5%. The deviation between most of the data by Kuznetsov and Los (1985; from TRC source 1996) and present correlation are less than 5% with some exceeding 5%. The differences between this correlation and the correlation by Defibaugh et al. (1994), the data by Zhang et al. (1995), and the data by Sato et al. (1994) are less than 3%. The extrapolated values at low temperatures using the correlation by Hozumi et al. (1994) differ significantly from our correlation with a maximum deviation exceeding 10%.

Acknowledgment

We are grateful to Dr. K. N. Marsh for providing the data from TRC database, and we are grateful to Zhejiang Fluoro-Chemical Technology Research Institute and U.S. EPA for providing the HFC-32 sample.

Literature Cited

- Bignell, C. M.; Dunlop, P. J. Second Virial Coefficients for Fluoromethanes and Their Binary Mixtures with Helium and Argon. *J. Chem. Eng. Data* **1993**, *38*, 139–140.
 Defibaugh, D. R.; Morrison, G.; Weber, L. A. Thermodynamic Properties of Difluoromethane. *J. Chem. Eng. Data* **1994**, *39*, 333–340.
 Ewing, M. B.; Goodwin, A. R. H.; McGlashan, M. L.; Trusler, J. P. M. Thermophysical properties of alkanes from speed of sound deter-

- mined using a spherical resonator. 1. Apparatus, acoustic model, and results for dimethylpropane. *J. Chem. Thermodyn.* **1987**, *19*, 721–739.
- Ewing, M. B.; Goodwin, A. R. H.; McGlashan, M. L.; Trusler, J. P. M. Thermophysical properties of alkanes from speed of sound determined using a spherical resonator, 2. *n*-Butane. *J. Chem. Thermodyn.* **1988**, *20*, 243–256.
- Ewing, M. B.; Goodwin, A. R. H.; Trusler, J. P. M. Thermophysical properties of alkanes from speed of sound determined using a spherical resonator, 3. *n*-Pentane. *J. Chem. Thermodyn.* **1989**, *21*, 867–877.
- Gallagher, J.; McLinden, M.; Morrison, G.; Huber, M. *NIST Thermodynamic Properties of Refrigerants and Refrigerants Mixtures, Version 4.01*; NIST Standard Reference Database 23, 1989.
- Goodwin, A. R. H.; Moldover, M. R. Thermophysical Properties of Gaseous Refrigerants from Speed of Sound Measurement. 1. Apparatus, Model and Results for 1,1,1,2-Tetrafluoroethane R134a. *J. Chem. Phys.* **1990**, *93*, 2741–2753.
- He, X. Y.; Zhao, Y. F. *Fundamentals of Acoustical Theory*, National Defense Industry Publishing House: Beijing, China, 1980.
- Hirschfelder, J. O.; Curtiss, C. F.; Bird, R. B. *Molecular Theory of Gases and Liquids*; Wiley: New York, 1954.
- Hozumi, T.; Sato, H.; Watanabe, K. Speed of Sound in Gaseous Difluoromethane. *J. Chem. Eng. Data* **1994**, *39*, 493–495.
- JANAF Thermophysical Tables. *J. Phys. Chem. Ref. Data* **1985**, *14*, Suppl. 1.
- Kubota, H.; Sotani, T.; Kunimoto, Y. Isobaric Specific Heat Capacity of Difluoromethane at Pressure up to 0.5 MPa. *Fluid Phase Equilib.* **1995**, *104*, 413–419.
- Kuznetov, A. P.; Los, L. V. Thermophysical Properties of Freons Calculation of Thermodynamic Properties of Difluoromethane (Freon 32). *Kholod. Tekh. Tekhnol.* **1985**, *14*, 40–43.
- McLinden, M. O. Thermodynamic Properties of CFC Alternatives: A Survey of the Available Data. *Int. J. Refrig.* **1990**, *13*, 149–161.
- Qian, Z. Y.; Nishimura, A.; Sato, H.; Watanabe, K. Compressibility Factors and Virial Coefficients of Difluoromethane (HFC-32) Determined by Burnett Method. *JSME Int. J. Ser. B* **1993**, *36*, 665–670.
- Reid, R. C.; Herwood, T. K. *The Properties of Gases and Liquid*, 2nd ed.; McGraw-Hill: New York, 1966.
- Roders, A. S.; Chao, J.; Wilhot, C.; Zwolinaki, B. J. *J. Phys. Chem. Ref. Data* **1974**, *3*, 117–140.
- Sato, T.; Sato, H.; Watanabe, K. PVT Property Measurements for Difluoromethane. *J. Chem. Eng. Data* **1994**, *39*, 851–854.
- TRC Databases for Chemistry and Engineering-SOURCE Database, Version 1996-4*; Thermodynamics Research Center, Texas A&M University System: College Station, TX, 1996.
- TRC Databases for Chemistry and Engineering-Thermodynamic Tables, Version 1997-1S*; Thermodynamics Research Center, Texas A&M University System: College Station, TX, 1997; V-6880 (NH), 1989.
- Weber, L. A.; Goodwin, A. R. H. Ebulliometric Measurement of the Vapor Pressure of Difluoromethane. *J. Chem. Eng. Data* **1993**, *38*, 254–256.
- Zhang, L. H.; Sato, H.; Watanabe, K. Second Virial Coefficients for R32, R125, R134a, R143a, R152a and Their Binary Mixtures. *Conference of 19th International Congress of Refrigeration*; Hague, Netherlands; 1995, pp 622–629.
- Zhu, M. S.; Han, L. Z.; Zhang, K. Z.; Zhou, T. Y. Sound Velocity and Ideal-Gas Specific Heat of 1,1,1,2-Tetrafluoroethane. *Int. J. Thermophys.* **1993**, *14*, 1039–1050.

Received for review February 12, 1997. Accepted April 22, 1997.
This work was supported by the National Natural Science Foundation of China.

JE970035N

⊗ Abstract published in *Advance ACS Abstracts*, June 1, 1997.